

TRAIL Conjugated Silver Nanoparticle Synthesis, Characterization and Therapeutic Effects on HT-29 Colon Cancer Cells

Fatih Birtekocak^a, Gulen Melike Demirbolat^b and Ozge Cevik^{a*}

^aDepartment of Biochemistry, School of Medicine, Aydin Adnan Menderes University, Aydin, Turkey. ^bDepartment of Pharmaceutical Technology, Faculty of Pharmacy, Biruni University, Istanbul, Turkey.

Abstract

Colon cancer is one of the most prominent causes of cancer-related morbidity and mortality and curable if detected in the early stages. TNF-related apoptosis-inducing ligand (TRAIL) is a therapeutic protein and has a potential anti-cancer activity that is widely used for the treatment of several cancers. In this study, we aimed to develop a silver nanoparticle system conjugated with TRAIL and coated with PEG (AgCTP NPs) to improve the therapeutic effects of colon cancer. AgCTP NPs were characterized by UV spectrum, FTIR and zetasizer. Cytotoxicity, hemolysis assay and apoptotic effects of nanoparticles were investigated using a colon cancer cell line (HT-29) *in-vitro*. Treatment with AgCTP NPs effectively inhibited proliferation and colony formation of HT-29 cells. The apoptotic effects of nanoparticles on HT-29 cells were determined as Bax, Bcl-2, PARP and clv-PARP protein expression levels using Western blot. Apoptotic proteins were upregulated by AgCTP NPs. In this study, we demonstrated that AgCTP NPs had an anti-cancer effect by activating cell death. Thus, we have confirmed that silver nanoparticles can be selected as a good carrier for TRAIL therapeutic proteins that can be used to treat colon cancer.

Keywords: TRAIL; Colon Cancer; Silver Nanoparticles; Apoptosis; HT-29 cells.

Introduction

Colorectal cancer, commonly called colon cancer, is the third most widely diagnosed cancer worldwide and is highly preventable and curable if detected in the early stages (1, 2). There are many different colon cancer therapies, including surgery, chemotherapy and radiation therapy which is a complementary therapy. However, these therapies are usually inefficient due to non-effective anti-cancer agents in targeting sites (3). Because higher doses can also lead to adverse effects, it should not be used. In addition to cancerous cells, healthy cells are

also damaged in these processes. Therefore, alternative systems should be developed for effective dose delivery.

Nanotechnology, a multidisciplinary field covering many fields such as physics, chemistry, biology, engineering and medicine, has recently emerged as one of the most favorable areas for cancer treatment (4). It has an incredible potential to revolutionize drug delivery and delivery systems that represent the optimal application of nanoparticles (NPs) (5). Considering the chelating ability and workability of metal NPs, an effective dose amount can be delivered to the target site after therapeutic agents are loaded onto the NPs (6). Additionally, NPs tend to accumulate more in tumor tissue than in normal tissues via the

* Corresponding author:
E-mail: ozge.cevik@adu.edu.tr

enhanced permeability and retention (EPR) effect and can efficiently be taken up by the cells (7-9). Employing rationality of the EPR effect is that the NPs cannot pass through the openings of normal vessels, which are less than 10 nm in size and would enter the openings of the tumor vessels, which can be hundreds of nanometers (10). Therefore, NPs fascinate many researchers for drug delivery systems. Especially, gold and silver NPs have recently been used as drug carriers (11, 12). Silver NPs can also be used in medical imaging, biosensors, nanocomposites, antimicrobials and cell electrodes (13). It is known that silver has better light absorption compared to other metal ions so that better resolution and better affinity can be provided for functionality (14, 15).

TNF-related-apoptosis-inducing ligand (TRAIL) is a member of the tumor necrosis factor (TNF) superfamily (16). It was first cloned and identified in 1995 by Wiley *et al.* (17). TRAIL protein (theoretically about 23 kDa) contains 281 and 289 amino acid residues in the human and murine forms, respectively, both sharing 65% sequence identity (18). It is expressed on the surface of natural killer (NK), T cells, macrophages and dendritic cells (19). TRAIL can favorably induce apoptosis in various primary tumor cell lines such as colon, breast, lung, skin, thyroid, prostate, kidney, pancreas and central nervous system (20) through interacting with its proapoptotic death receptors (DR4 and DR5) (20, 21) but not in normal cells. Therefore, it has attracted a number of research laboratories and pharmaceutical companies, and they have desired to develop recombinant forms of TRAIL (rTRAIL) or TRAIL receptor agonists for therapeutic purposes (22).

TRAIL can induce apoptosis up to 5 ng/mL, but its biological half-life is quite short in rTRAIL (23-25). Namely, TRAIL has poor stability. Therefore, the effective dose amount of TRAIL cannot reach the tumor tissue (26). This disadvantage can be overcome by NPs having stability and EPR effect and/or through coating processes such as PEGylation, thereby enabling higher and effective dose delivery to the target site.

When NPs enter the body, they can inevitably interact with biological molecules

such as proteins to form the Corona or replace the existing ligand with other molecules (27). Therefore, NPs seem reasonable to cover with a coating material such as PEG. Additionally, it is widely reported that the PEGylated NPs have a “secret” character that can delay or prevent by the rapid cleaning of the reticuloendothelial system (RES) (28, 29). Furthermore, PEGylation improves the targeting of cancerous cells through the EPR effect (30).

Experimental

Materials And Methods

Design, Production, and Characterization of rTRAIL protein

TRAIL gene (Ensemble: ENSG00000121858) was amplified from human TRAIL cDNA. XhoI and NotI restrictions sites had been added at the 5'end of the forward and reverse primers, respectively, and their sequences were as follows: 5'ATGCCCTCGAGATAGAGAAGGAAGGGCTTCAGTG`3 and 5'ATGCGCGGCCCGTGCGATCTTTTAGTGGTGCCT`3.

Primer was designed and analyzed with software (Primer-BLAST, NCBI). The amplification of the human TRAIL gene was performed using DNA Polymerases (F530S Phusion High-Fidelity DNA Polymerases, Thermo Scientific) with PCR (T100 Thermal Cycler, Biorad). pET28a, his tagged bacterial expression plasmid (EMD Biosciences, USA), was digested with XhoI and NotI (R0146S and R0189S, New England Biolabs). Then TRAIL gene was ligated to pET28a and named pET28a.TRAIL. The pET28a.TRAIL expression plasmid was also transformed into *Escherichia Coli* (*E. coli*) BL21 (DE3). *E. coli* was cultured in LB with Kanamycin (Santa Cruz, USA) at 100 µg/mL, and recombinant protein expression was induced with 1 mM isopropyl β-d-1-thiogalactopyranoside (IPTG, Sigma). Recombinant TRAIL protein (rTRAIL) was purified on Ni-NTA affinity beads (Santa Cruz). Protein was controlled with 15% SDS-PAGE gels and staining Coomassie brilliant blue. Commercial TRAIL protein (Sigma T9701) was used as a positive control to TRAIL purification.

Synthesis of silver nanoparticles

After the magnetic stirrer was adjusted to 37 °C, 100 mL of met-NaOH (0.02 M, 99%) solution and 1 mL of cysteine solution (0.1 M) were added in a 250 mL beaker. pH was adjusted to 9 by 1M HCl and 2N NaOH, and then 1 mL of AgNO₃ (0.1 M) solution was added dropwise to this mixture. One-hundred µL TRAIL (20 µg/mL) and 100 µL PEG₄₀₀ were respectively added in the same way after every 10 min and stirred for 4 h. The mixture was centrifuged for 5 min at 4000 rpm (Hettich 320R, Germany). To remove impurities, the pellet was separately washed 3 times with methanol and dH₂O. The powder form of nanoparticles obtained by lyophilization and was kept at 4 °C for further studies. AgC (Silver-cysteine), AgCT (Silver-cysteine-TRAIL) and AgCTP (Silver-cysteine-TRAIL-PEG) NPs were synthesized by the same procedure.

Characterization of silver nanoparticles

Polarized light-absorbing properties of AgCT NPs were examined by Ultraviolet-visible (UV-Vis) spectrophotometer (Thermo Scientific Multiskan Spectrum 1500, USA) with a range of 200-800 nm. The functional groups of AgCT NPs were confirmed by Fourier-transform infrared (FTIR) spectroscopy in the range of 650-4000 cm⁻¹ (PerkinElmer UATR two, U.S.). Particle size and zeta potential values of the synthesized AgCT NPs were determined by Zetasizer (Nano ZS-90 Malvern Instruments, England).

Cell culture and cell survival assay

HT-29 human colon cancer cell lines were purchased from the American Type Culture Collection (ATCC, Manassas, VA, USA). These cells were cultured in Dulbecco's Modified Eagle's Medium (DMEM) supplemented with 10% FBS, 2 mM L-glutamine, 100 U/mL penicillin and 100 µg/mL streptomycin, and kept at 37 °C under 5% CO₂. To determine the cell viability, cells were trypsinized and seeded into 96-well plates (1 × 10⁴ cells/well). The cells were treated with different concentrations (1.56–25 ng/mL) of AgCT NPs. Control cells were incubated without AgCT NPs. All wells were incubated for 24 h, then washed with PBS and added to

100 µL DMEM. For MTT assay, ten microliter of the MTT (3-(4,5-dimethylthiazol-2-yl)-2,5-diphenyltetrazolium bromide) (Vybrant, Invitrogen) labeling reagent was added to this wells and incubated for 4 h in a humidified atmosphere at 37 °C incubators with 5% CO₂ in the air. After the incubation, 100 µL of the SDS buffer was added into each well for solubilization of formazan precipitate. Then absorbance was measured by microplate reader at 570 nm (Thermo Scientific Multiskan Spectrum 1500, USA). Each analysis was repeated 3 times. Cell viability was calculated as follows:

$$\text{Cell viability\%} = \frac{(\text{Abs}_{(\text{sample})} - \text{Abs}_{(\text{blank})})}{(\text{Abs}_{(\text{control})} - \text{Abs}_{(\text{blank})})} \times 100$$

Cell growing assay

In order to investigate the effects of AgCT NPs on cell survival of HT-29 cells, these cells were treated with AgCT NPs, a final concentration of 1.19 ng/mL, in DMEM without antibiotics. In microscopic analysis, images were collected under an inverted microscope (Olympus CX51) with bright light. After 24 h, methylene blue staining was used in cell viability for Microscopic analysis. The cells extracted with 1% SDS in PBS solution were stained with 0.01% methylene blue solution and then spectrophotometrically was evaluated at 600 nm. Each experiment was repeated three times.

Colony formation assay

For evaluating colony formation, HT-29 cells seeded in six-well plates (1000 cells per well) were treated with AgCT NPs and cultured in a growth medium for 14 days. The medium was refreshed every 3 days until incubation was completed. At the end of incubation, each well in the plate was washed with PBS, fixed with cold methanol/acetic acid, stained with 0.5% crystal violet staining solution for 15 min and washed with dH₂O, respectively. The stained cells were examined with a microscope. The number of colonies in each well was counted and analyzed.

Hemolysis Assay

The freshly obtained blood sample was put

into tubes involving EDTA and centrifuged at 1000 ×g for 15 min. After discarding the supernatant, 10% (w/v) RBC solution was prepared with pellet in PBS (pH 7.4). One-hundred μL RBC solution and 900 μL AgCT NPs with different concentrations (25, 12.5 and 6.25 ng/mL) were mixed in a microtube and then were incubated at 37 °C for 1 h. By the way, 900 μL 0.9% NaCl and dH₂O were used for negative and positive control, respectively. The mixtures were centrifuged at 1000 ×g for 15 min following incubation and supernatants were spectrophotometrically measured at 540 nm. The experiments were repeated three times. The percentage of hemolysis was calculated as follows:

$$\text{Hemolysis\%} = \frac{(\text{Abs}_{(\text{sample})} - \text{Abs}_{(-\text{control})}) / (\text{Abs}_{(+\text{control})} - \text{Abs}_{(-\text{control})}) \times 100$$

According to this formula, the negative control was accepted as blank.

Western blot analysis

HT-29 cells were lysed with RIPA buffer after incubation with AgCT NPs. Protein detection was performed with bicinchoninic acid assay (BCA) and then 30 μg protein was loaded per well in 12% SDS-PAGE gel. Proteins were separated by SDS-PAGE and transferred onto PVDF membrane (sc-3723, Santa Cruz). The membrane was blocked with 3% BSA for 2 h at room temperature and then was incubated with primary antibodies (1:500 dilution of Bax, Bcl-2, PARP, clv-PARP and β-actin from Santa Cruz) at 4 °C overnight. After the incubation with primary antibody, PVDF membrane was washed with TBST (Tris-buffered saline, 0.1% Tween 20) and incubated with horseradish peroxidase-conjugated secondary antibody (mouse anti-rabbit IgG-HRP and goat anti-mouse IgG₁-HRP from Santa Cruz) for 2 h at room temperature. Then the membrane was washed with TBST. Bands were visualized by the chemiluminescence Western blotting detection reagent (sc-2048, Santa Cruz) in imaging system (G:BOX Chemi XRQ SynGene, USA). β-Actin protein levels were used as a control to equal loading of the gel. The experiments were repeated three times.

Statistical analysis

The student *t*-test and analyses of variance (ANOVA) test were used for statistical analysis. If the *p*-value which is used to determine the level of statistical significance and difference, was equal to 0.05 or less than 0.05, it was considered significant. All data were represented as mean ± SD unless otherwise indicated. All experiments were repeated three times.

Results

Synthesis of Silver Nanoparticles

The purpose of the presented studies was to obtain TRAIL conjugated silver nanoparticles dedicated for colon cancer therapy. Because the sulfur end of cysteine was negatively charged due to the deprotonation of sulfur moiety, pH was chosen as 9.00. Thus, the synthesized AgC molecules were bounded with an Ag-S chemical bond. However, AgC molecules were coated with TRAIL to form AgCT molecules by hydrogen bonds. PEG molecules in AgCTP NPs were also bonded to AgCT NPs by a hydrogen bond. Figure 1 shows the synthesis steps of AgCTP NPs.

Characterization of synthesized AgNPs

Normally, silver(I) nitrate react with sodium hydroxide to produce silver(I) oxide by the reaction: $2\text{AgNO}_3 + 2\text{NaOH} \rightarrow \text{Ag}_2\text{O} + 2\text{NaNO}_3 + \text{H}_2\text{O}$

Silver oxide is a black or dark brown color and slightly soluble in water. However, the AgCT NPs which we synthesized were light brown and had good water solubility. Based on this informations and our previous experiences, we are confident that synthesized AgCT NPs were different molecules from Ag₂O.

The color change is usually occurring in the synthesis of metal NPs, so visual observation is a good sign of metal NPs synthesis. During the synthesis, this change is caused by the excitation of the surface plasmon resonance (SPR) effect on metal NPs. Our experiments showed that the appearance of a light brown color was evidence of the formation of the AgNPs. In addition to quantitative results, we also performed qualitative assessments to confirm the synthesis of AgNPs. The supernatant and pellet for AgC binding control

were subjected to a modified ninhydrin test. The modified ninhydrin test is specific to amino acids (31). Namely, this test can be used to verify the absence or presence of amino acids. The pellet had a purple-red color for the ninhydrin test, while the supernatant had a clear color (Supplementary file, Figure S1a). The result of this test was positive only for pellet. According to the ninhydrin experiment results for pellet of AgC NPs, Ag and cysteine were in the same environment. However, the main problem was whether they were bonded by the Ag-S chemical bonding. Therefore, we used the nitroprusside test. The nitroprusside test is positive for the presence of free -SH group, but it was negative for pellet of AgC NPs (Supplementary file, Figure S1b). Obviously, the free -SH end in the cysteine lost proton and interacted with Ag to form the Ag-S chemical bonding.

In this study, TRAIL expression by *E. coli* BL21(DE3) was generated by pET28a. TRAIL vector. The pET28a. TRAIL vector is predicted to encode a recombinant protein with a molecular size of 24 kDa in the induction of IPTG (Supplementary file, Figure S1c). To check whether TRAIL binds to AgC NPs, the Bradford test was used in the AgCT NPs. The Bradford test is one of the methods used to verify the presence of proteins and to calculate protein quantity up to 1 microgram. The test result for AgCT NPs was positive

in both pellet and supernatant of AgCT (Supplementary file, Figure S1d). However, in our preliminary trials, only the supernatant of AgCTP was negative. The pellet for AgCT NPs had dark blue color, but the supernatant had a light blue. Additionally, OD_{595} values were 0.089 ± 0.012 (AgCT pellet) and 0.023 ± 0.007 (AgCT supernatant). When the standard chart was drawn against BSA, the amount of free TRAIL found about 0.2 μg . It was quite normal because some of TRAIL might have released from AgCT NPs due to centrifugal forces, and/or some of the TRAIL might not have bounded to AgC NPs. According to the gel electrophoresis results, we could not observe a single TRAIL band other than AgCT and AgCTP NPs bands (Supplementary file, Figure S1e). This means that free TRAIL molecules were removed from AgCT and AgCTP NPs as much as possible during the washing of Ag NPs pellet. In addition, the presence of TRAIL bands of AgCT and AgCTP molecules at different locations in gel electrophoresis indicates that the AgCTP molecule was correctly pegylated.

Figure 2a shows UV-Vis spectra from different AgNPs. These spectrums indicated the formation of AgC, AgCT and AgCTP NPs, which were different from each other. The absorption spectrum of AgCT and AgCTP NPs spanned a wide range from 200 to 700 nm with a prominent peak at 389. However, AgC NPs had a prominent peak at 385.

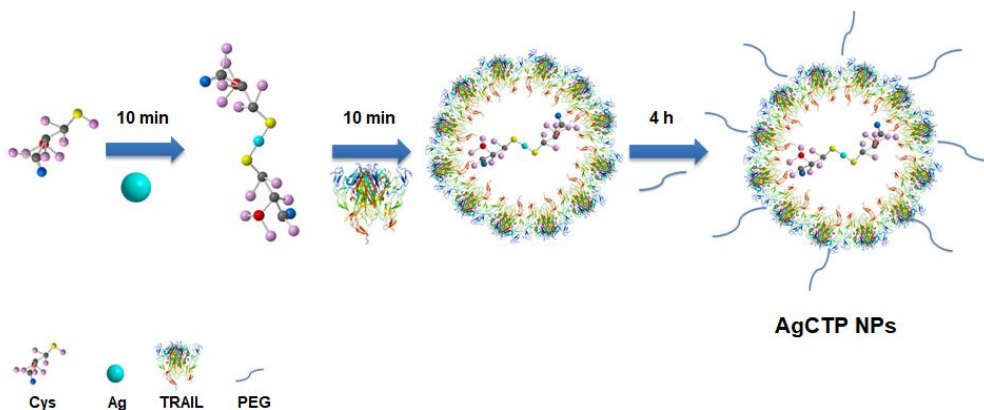


Figure 1. Schematic representation of synthesis AgCTP nanoparticles.

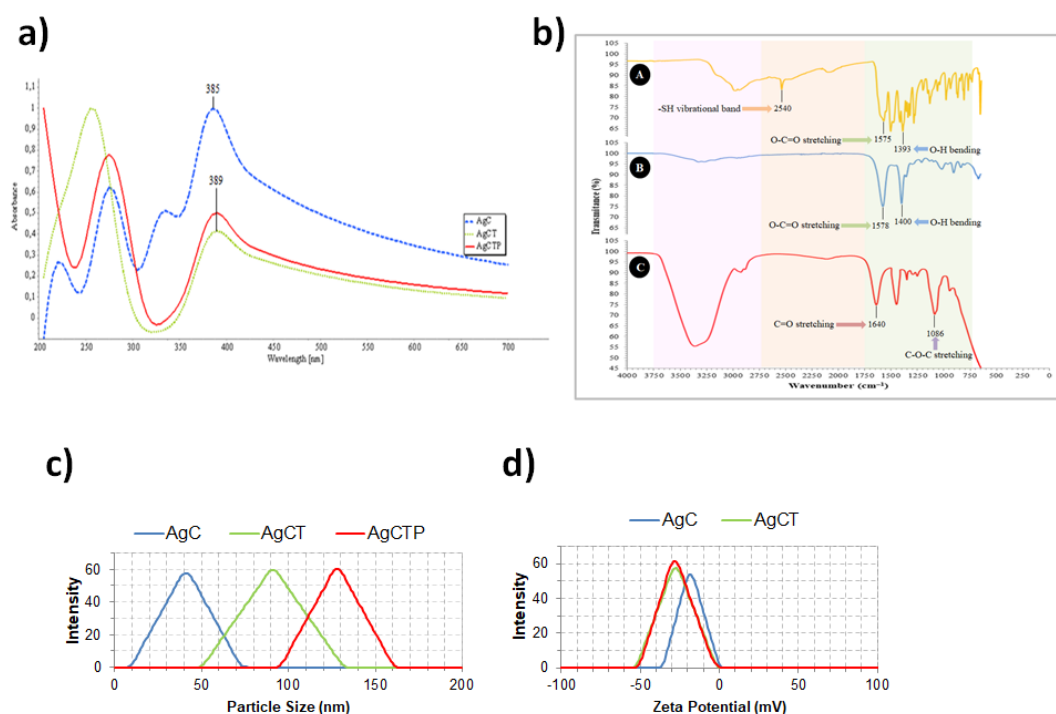


Figure 2. Characterization of AgCT NPs conjugated with TRAIL, (a) UV-Vis spectrum of AgNPs, (b) FTIR spectrum of cysteine (A), AgC (B) and AgCTP (C) molecules FT-IR spectrum (c), particle characterization, (d) zeta potential.

The prominent –SH vibrational band at 2540 cm^{-1} in the FTIR spectrum was clearly appeared in the free cysteine molecule but not in the AgC and AgCTP (Figure 2b). The lack of the band at 2540 cm^{-1} showed the formation of Ag–S covalent bond in the AgC and AgCTP NPs (32, 33). According to the literature data, the characteristic vibrational band of Ag–S is observed at $\sim 210\text{--}245\text{ cm}^{-1}$ (34). We could not observe this peak due to the detection limits of the device we use. The carboxylate stretching vibration of the cysteine and AgC molecules were respectively observed at 1575 cm^{-1} and 1578 cm^{-1} (33). The hydroxyl bending vibrations, with carboxylic acid, the cysteine and AgC molecules were observed at 1393 cm^{-1} and 1400 cm^{-1} . A peptide bond is an amide-type of the covalent chemical bond, and it is one of the best indicators of protein presence. The peak of amide for the TRAIL protein (C=O stretching) was observed at 1640 cm^{-1} for AgCTP molecule (Figure 2b) (35). However,

the ether stretching vibration for PEG was observed at 1086 cm^{-1} (36, 37).

Particle sizes of AgNPs were found as $41.21 \pm 3.80\text{ nm}$ (AgC), $91.22 \pm 7.34\text{ nm}$ (AgCT) and $128.12 \pm 8.02\text{ nm}$ (AgCTP) (Figure 2c). However, zeta potential values of AgNPs were measured $-19.22 \pm 3.07\text{ mV}$ (AgC), $-27.3 \pm 4.34\text{ mV}$ (AgCT) and $-28.75 \pm 2.02\text{ mV}$ (AgCTP) (Figure 2d).

Cell viability, proliferation and hemocompatibility with AgNPs

HT-29 cells were treated with AgNPs at different concentrations ($1.56\text{--}25\text{ ng/mL}$) for 24 h, and cytotoxicity analysis was determined using MTT assay. Figure 3a shows, AgC did not produce a significant reduction in viability of HT-29 cells. However, AgCT up to 12.5 ng/mL and AgCTP up to 6.25 ng/mL did not significantly reduce the viability of HT-29 cells. Especially, this reduction was 2.5 fold in AgCTP at 25 ng/mL compared to control. Moreover, AgCTP NPs generally showed

more decrease in cell viability than AgCT NPs.

The behavior of AgNPs under physiological conditions, with a non-toxic effect, was promising for *in-vivo* applications. Figure 3b shows the hemolysis rate for the AgNPs (25 ng/mL). The results have shown that the hemolysis rates for the AgNPs were statistically significant according to positive controls and were almost equivalent to negative controls.

It was possible to associate further decline with the EPR effect. Because the total cell count significantly reduced after 24 h treatment with 25 ng/mL AgCT and AgCTP NPs, microscopic evaluations for morphological changes were also made (Figure 3c). AgCTP NPs treated cells showed loss of membrane integrity, cell growth inhibition, cytoplasmic condensation, creating curved forms, and apoptosis body.

The control cells showed cell-cell interaction via normal morphological alterations. The concentration of 25 ng/mL AgCT and AgCTP NPs showed an antiproliferative effect on the proliferation of colon cancer cells compared to control (Figure 3d).

The colony-forming ability of HT-29 cells with AgNPs treatment

The colony-forming ability of HT-29 cells was evaluated in cell culture by treatment of AgNPs. Twenty-five ng/mL AgCT or AgCTP NPs showed a significant decrease in the number of colon cancer cell colonies compared to control. However, there was no significant reduction in treatment with 25 ng/mL AgC compared to control. These data have shown that AgCT and AgCTP NPs diminished the metastatic effect by carrying out TRAIL proteins on HT-29 colon cancer cells (Figures 3e-3f).

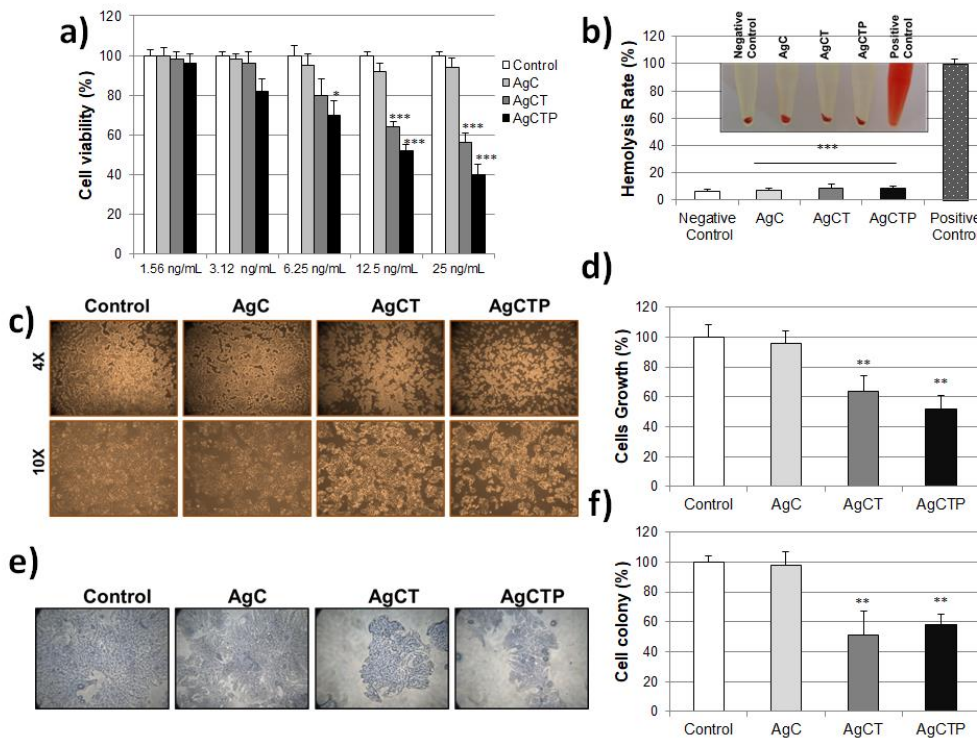


Figure 3. (a) Cell viability measurement with MTT assay after AgCT NPs treatment (1.56–25 ng/mL) of HT-29 cell lines for 24 h. (b) *In-vitro* hemolysis assay of AgNPs in red blood cells. The ratio of hemolysis in red blood cells with treated AgCT NPs ($***p < 0.001$ compare to positive control). Effect of AgCT NPs (25 ng/mL) on the cell survival in HT-29 human colon cancer cells for 24 h (c) Cell morphological changes (d) Ratio of cell growing ($**p < 0.01$ compare to control) (e) Cell colony formation stained with crystal violet (f) Ratio of cell colony ($**p < 0.01$ compare to control) (Results are representative of three biological replicates).

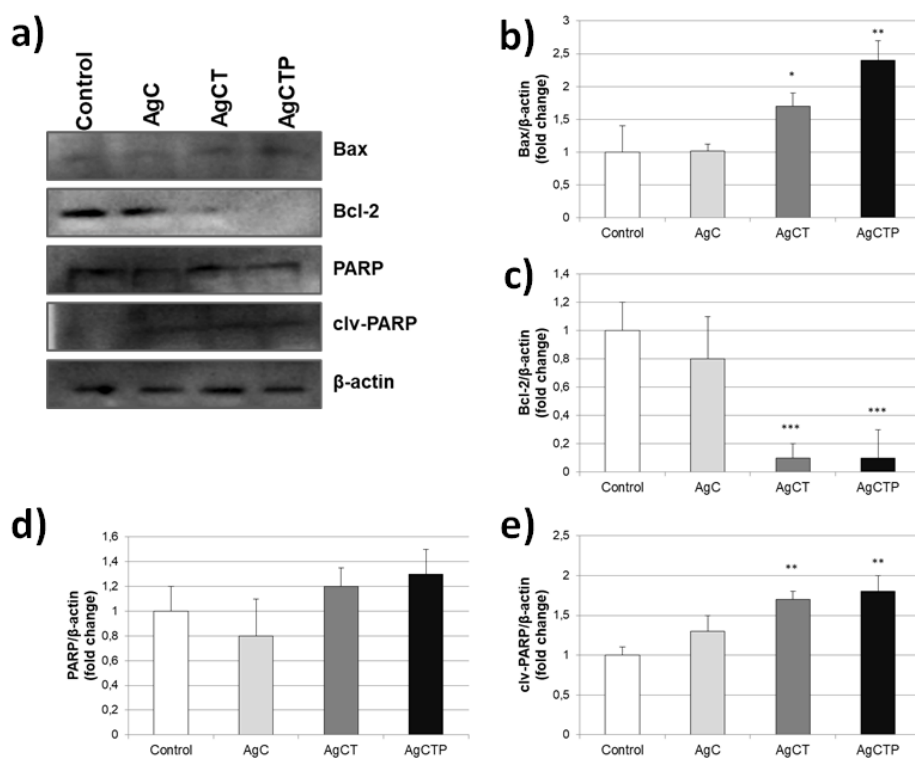


Figure 4. Effects of AgCT NPs (25 ng/mL) on apoptotic and anti-apoptotic proteins in HT-29 human colon cancer cells for 24 h. (a) Western blot bands of expression levels of Bax, Bcl-2 and PARP proteins. Each protein band was normalized to the intensity of β -actin used. Western blot densitometry analysis of (b) Bax (c) Bcl-2 (d) PARP (e) clv-PARP protein expression levels. (* $p < 0.05$, ** $p < 0.01$, *** $p < 0.001$ compare to control cells, (Results are representative of three biological replicates).

Cell apoptosis with AgNPs

To investigate the effects of AgNPs on apoptosis in HT-29 cell line, these cells were treated with 25 ng/mL AgNPs for 24 h and then the expression levels of Bax, Bcl-2, PARP, clv-PARP and β -actin (control) proteins were assessed by western blot. Our results showed that AgC NPs had no significant effect on apoptosis (Figures 4a-4e). However, AgCT and AgCTP NPs showed statistically significant differences in Bax, Bcl-2 and clv-PARP expression levels except PARP proteins involved in apoptosis regulation.

Discussion

The functionalization of AgNPs with therapeutic increases efficacy in targeted drug delivery in cancer, improving the efficacy of nanomedicine-based theranostics applications. Today, AgNPs play a special role in cancer

therapy because of their unique physical and chemical properties.

AgNPs surface layer may be functionalized with various chemical functional groups or moieties to enhance binding drug or proteins. Surface functionalization of silver nanoparticles can be performed by cysteine that changes some characteristic features of silver nanoparticles. Most publications have reported that the characteristic peak around 400-450 nm seen in the UV-vis spectrum is specific for AgNPs (38, 39). As cysteine was not used as a functional group in these publications, it was normal to observe characteristic peaks around 400-450 nm for AgNPs. But there are also publications similar to our results indicating that the characteristic peak was about 390 nm. In these publications, cysteine was used as a functional group to form AgNPs (34, 40-42).

The particle size of the NPs is an important factor affecting the delivery of therapeutic agents to solid tumors. It has been reported that NPs larger than 500 nm are rapidly cleared from the body by the macrophage and monocytes of RES while particles smaller than 10 nm can undergo renal clearance; larger than 200 nm can experience splenic clearance (43,44). Therefore, it is possible to say that NPs less than 200 nm are the most suitable for intravenous applications (45). However, 341.6 nm-sized TRAIL/Dox HSA-NPs have been shown to be effective for lung cancer *in-vitro* and *in-vivo* by aerosolization (46). If we look at the size of synthesized AgC, AgCT and AgCTP NPs, they were 41 nm, 91 nm and 128 nm, respectively. Since additional groups were added to the molecule, particle size increased. For example, spherical structures of TRAIL NPs and TRAIL-PEG NPs, with heparin and poly-L-lysine, were stated to have a size of 205.4 and 213.3 nm, respectively. Despite this size, TRAIL-PEG NPS was stable in circulation for a long time compared to TRAIL (47). In addition, NPs with zeta potential value greater than ± 30 mV as numeric are considered highly stable in the dispersion medium (48). Thus, our synthesized AgCTP NPs may remain stable *in-vitro* and/or *in-vivo* for a long time.

TRAIL is a safe, powerful and well-tolerated anti-cancer agent. It can induce apoptosis by using an extrinsic pathway via the proapoptotic death receptors (DR4 and DR5) in cancer cells but not in normal cells (49). Therefore, it has also been used in many clinical trials as well as *in-vitro* studies (50-54). However, TRAIL use in the clinic is not suitable because of its short biological half-life, which was started approximately 0.5 to 1 h (51). Because the amount of dose that TRAIL is effective cannot be delivered into the tumor tissue. Therefore, TRAIL has commonly used in combination with other anti-cancer agents to create a synergistic effect (55-60). Whereas the power of TRAIL can be revealed by coating with materials such as PEG (53, 61 and 62) and/or by functioning with NPs (26, 63 and 64) without the need for combined treatments. For example, Kim and *et al.* have shown that PEGylated TRAIL molecules have long-term activity proportional to the molecular weight

of PEG (61). Lim *et al.* have emphasized that TRAIL-PEG-NPs formulation extended the half-life of TRAIL by 28.3 fold in rats (62). In the xenograft mouse model with a similar strategy, it was observed that serum half-life of the human serum albumin (HSA)-TRAIL increased 15 fold compared to rTRAIL (65). By Bae and *et al.*, TRAIL/Transferrin/Dox HSA-NPs were found to be retained in circulation for 32 h (66). Additionally, it is stated that TRAIL-loaded poly(lactic-co-glycolic acid) microspheres showed sustained TRAIL release for up to 10 days *in-vivo* xenograft tumor model (67). The main purpose of synthesized AgCT NPs coating with PEG was to prolong the half-life of AgCT NPs. Furthermore, PEGylation improved targeting to cancerous cells by the EPR effect and would prevent AgCT NPs from interacting with other molecules in circulation.

In studies conducted with TRAIL, it has been observed that Bcl-2 protein is generally overexpressed due to the non-effective dose of anti-cancer agent and thus improves resistance to apoptosis. In a study by Rudner and *et al.*, it has been shown that TRAIL up to 10 ng/mL increased expression of Bcl-2 despite tetracycline-repressed Bcl-2 (68). Meanwhile, HT-29 cancer cells underwent apoptosis by increased Bax expression and loss of Bcl-2 after treatment with AgCTP NPs (25 ng/mL). Increased Bax level is a clear sign of apoptosis, while decreased Bcl-2 level indicates no resistance to apoptosis.

As a result, we suggest that cysteine, PEG and TRAIL conjugated AgCTP NPs can be used as a safe and effective anti-cancer agent. Considering hemolysis assay results, this conjugation can also be used *in-vivo* studies without creating a toxic effect.

Acknowledgments

This work was supported by Adnan Menderes University Research Grant (ADU-TPF-18012) and by a partly grant (214Z057) from the Scientific and Technological Research Council of Turkey (TUBITAK) and to Dr. Ozge Cevik. The analysis conducted by the Adnan Menderes University Science and Technology Research Center (ADU-BILTEM) is gratefully acknowledged.

References

- (1) Chen W, Zheng R, Baade PD, Zhang S, Zeng H, Bray F, Jemal A, Yu XQ and He J. Cancer statistics in China, 2015. *CA Cancer J. Clin.* (2016) 66: 115–32.
- (2) Siegel RL, Miller KD and Jemal A. Cancer Statistics, 2017. *CA Cancer J. Clin.* (2017) 67: 7–30.
- (3) Hamzehzadeh L, Imanparast A, Tajbakhsh A, Rezaee M and Pasdar A. New Approaches to Use Nanoparticles for Treatment of Colorectal Cancer; A Brief Review. *Nanomed. Res. J.* (2016) 1: 59-68.
- (4) Sengupta S, Eavarone D, Capila I, Zhao G, Watson N, Kiziltepe T and Sasisekharan R. Temporal targeting of tumour cells and neovasculature with a nanoscale delivery system. *Nature* (2005) 436: 568–72.
- (5) Parveen S and Sahoo SK. Polymeric nanoparticles for cancer therapy. *J. Drug Target* (2008) 16: 108–23.
- (6) Zalba S, Contreras AM, Haeri A, Ten Hagen TL, Navarro I, Koning G and Garrido MJ. Cetuximab-oxaliplatin-liposomes for epidermal growth factor receptor targeted chemotherapy of colorectal cancer. *J. Control. Release* (2015) 210: 26-38.
- (7) Demirbolat GM, Altintas L, Yilmaz S and Degim IT. Development of orally applicable, combinatorial drug-loaded nanoparticles for the treatment of Fibrosarcoma. *J. Pharm. Sci.* (2018) 107: 1398-407.
- (8) Ngoune R, Peters A, von Elverfeldt D, Winkler K and Pütz G. Accumulating nanoparticles by EPR: A route of no return. *J. Control Release* (2016) 238: 58–70.
- (9) Naoum GE, Tawadros F, Farooqi AA, Qureshi MZ, Tabassum S, Buchsbaum DJ and Arafat W. Role of nanotechnology and gene delivery systems in TRAIL-based therapies. *Ecancermedalscience* (2016) 10: 660.
- (10) Stylianopoulos T. EPR-effect: utilizing size-dependent nanoparticle delivery to solid tumors. *Ther. Deliv.* (2013) 4: 421-3.
- (11) Goyal G, Hwang J, Aviral J, Seo Y, Jo Y, Son J and Choi J. Green synthesis of silver nanoparticles using β -glucan, and their incorporation into doxorubicin-loaded water-in-oil nanoemulsions for antitumor and antibacterial applications. *J. Ind. Eng. Chem.* (2017) 47: 179–86.
- (12) Mirza AZ and Shamshad H. Fabrication and characterization of doxorubicin functionalized PSS coated gold nanorod. *Arab. J. Chem.* (2019) 12: 146-50.
- (13) Abbasi E, Milani M, Aval SF, Kouhi M, Akbarzade A, Nasrabadi HT, Nikasa P, Joo SW, Hanifehpour Y, Nejati-Koshki K and Samiei M. Silver nanoparticles: synthesis methods, bio-applications and properties. *Crit. Rev. Microbiol.* (2016) 42: 173-80.
- (14) Nedelcu IA, Ficai A, Sonmez M, Ficai D, Oprea O and Andronescu E. Silver based materials for biomedical application. *Curr. Org. Chem.* (2014) 18: 173-84.
- (15) Erdogan Ö, Abbak M, Demirbolat GM, Birtekocak F, Aksel M, Pasa S and Cevik Ö. Green synthesis of silver nanoparticles via *Cynara scolymus* leaf extracts: The characterization, anticancer potential with photodynamic therapy in MCF7 cells. *PLoS ONE* (2019) 14: e0216496.
- (16) Lafont E, Hartwig T and Walczak H. Paving TRAIL's Path with Ubiquitin. *Trends Biochem. Sci.* (2018) 43: 44-60.
- (17) Wiley SR, Schooley K, Smolak PJ, Din WS, Huang CP, Nicholl JK, Sutherland GR, Smith TD, Rauch C, Smith CA and Goodwin RG. Identification and characterization of a new member of the TNF family that induces apoptosis. *Immunity* (1995) 3: 673–82.
- (18) Jiang W, Wu DB, Fu SY, Chen EQ, Tang H and Zhou TY. Insight into the role of TRAIL in liver diseases. *Biomed. Pharmacother.* (2019) 110: 641–5.
- (19) Thorburn A. Tumor necrosis factor-related apoptosis-inducing ligand (TRAIL) pathway signaling. *J. Thorac. Oncol.* (2007) 2: 461-5.
- (20) Naimi A, Movassaghpour AA, Hagh MF, Talebi M, Entezari A, Jadidi-Niaragh F and Solali S. TNF-related apoptosis-inducing ligand (TRAIL) as the potential therapeutic target in hematological malignancies. *Biomed. Pharmacother.* (2018) 98: 566–76.
- (21) Schneider P, Bodmer JL, Thome M, Hofmann K, Holler N and Tschopp J. Characterization of two receptors for TRAIL. *FEBS Lett.* (1997) 416: 329-34.
- (22) Amarante-Mendes GP and Griffith TS. Therapeutic applications of TRAIL receptor agonists in cancer and beyond. *Pharmacol. Ther.* (2015) 155: 117–31.
- (23) Szliszka E, Kawczyk-Krupka A, Czuba ZP, Sieron A and Krol W. Effect of ALA-mediated photodynamic therapy in combination with tumor necrosis factor-related apoptosis-inducing ligand (TRAIL) on bladder cancer cells. *Cent. European J. Urol.* (2011) 64: 175-9.
- (24) Mitchell MJ, Wayne E, Rana K, Schaffer CB and King MR. TRAIL-coated leukocytes that kill cancer cells in the circulation. *Proc. Natl. Acad. Sci. U.S.A.* (2014) 111: 930-5.
- (25) Lawrence D, Shahrokh Z, Marsters S, Achilles K, Shih D, Mounho B, Hillan K, Totpal K, DeForge L, Schow P, Hooley J, Sherwood S, Pai R, Leung S, Khan L, Gliniak B, Bussiere J, Smith CA, Strom SS, Kelley S, Fox JA, Thomas D and Ashkenazi A. Differential hepatocyte toxicity of recombinant Apo2L/TRAIL versions. *Nat. Med.* (2001) 7: 383-5.

- (26) Perlstein B, Finnis SA, Miller C, Okhrimenko H, Kazimirsky G, Cazacu S, Lee HK, Lemke N, Brodie S, Umansky F, Rempel SA, Rosenblum M, Mikklesen T, Margel S and Brodie C. TRAIL conjugated to nanoparticles exhibits increased anti-tumor activities in glioma cells and glioma stem cells *in-vitro* and *in-vivo*. *Neuro Oncol.* (2013) 5: 29-40.
- (27) Cai C, Wang M, Wang X, Wang B, Chen H, Chen J, Chen C and Feng W. Transferrin adsorbed on PEGylated gold nanoparticles and its relevance to targeting specificity. *J. Nanosci. Nanotechnol.* (2018) 18: 5306–13.
- (28) Swierczewska M, Lee K and Lee S. What is the future of PEGylated therapies? Expert Opin. *Expert Opin. Emerg. Drugs* (2015) 20: 531–6.
- (29) Suk JS, Xu Q, Kim N, Hanes J and Ensigen LM. PEGylation as a strategy for improving nanoparticle-based drug and gene delivery. *Adv. Drug Deliv. Rev.* (2016) 99: 28–51.
- (30) de Miguel D, Lemke J, Anel A, Walczak H and Martinez-Lostao L. Onto better TRAILs for cancer treatment. *Cell Death Differ.* (2016) 23: 733-47.
- (31) Gaitonde MK. A Spectrophotometric Method for the Direct Determination of Cysteine in the Presence of Other Naturally Occurring Amino Acids. *Biochem. J.* (1967) 104: 627-33.
- (32) Pakhomov PM, Ovchinnikov MM, Khizhnyak SD, Lavrienko MV, Nierling W and Lechner MD. Study of Gelation in Aqueous Solutions of Cysteine and Silver Nitrate. *Colloid J.* (2004) 66: 65–70.
- (33) Jing C and Fang Y. Experimental (SERS) and theoretical (DFT) studies on the adsorption behaviors of L-cysteine on gold/silver nanoparticles. *Chem. Phys.* (2007) 332: 27–32.
- (34) Csapó E, Patakfalvi R, Hornok V, Tóth LT, Sipos A, Szalai A, Csete M and Dékány I. Effect of pH on stability and plasmonic properties of cysteine-functionalized silver nanoparticle dispersion. *Colloids Surf. B Biointerfaces* (2012) 98: 43-9.
- (35) Dutt A and Upadhyay LSB. Synthesis of Cysteine Functionalized Silver Nanoparticles using Green Tea Extract with Application for Lipase Immobilization. *Anal. Lett.* (2018) 51: 1071-86.
- (36) Feng C, Han X, Chi L, Sun J, Gong F and Shen Y. Synthesis, characterization, and *in-vitro* evaluation of TRAIL-modified, cabazitaxel-loaded polymeric micelles for achieving synergistic anticancer therapy. *J. Biomater. Sci. Polym. Ed.* (2018) 29: 1729-44.
- (37) Shameli K, Ahmad MB, Jazayeri SD, Sedaghat S, Shabanzadeh P, Jahangirian H, Mahdavi M and Abdollahi Y. Synthesis and Characterization of Polyethylene Glycol Mediated Silver Nanoparticles by the Green Method. *Int. J. Mol. Sci.* (2012) 13: 6639-50.
- (38) Marsich L, Bonifacio A, Mandal S, Krol S, Beleites C and Sergio V. PolyLlysine-Coated Silver Nanoparticles as Positively Charged Substrates for Surface-Enhanced Raman Scattering. *Langmuir* (2012) 28: 13166-71.
- (39) Gloria EC, Ederley V, Gladis M, César H, Jaime O, Oscar A, José IU and Franklin J. Synthesis of silver nanoparticles (AgNPs) with antibacterial activity. *J. Phys. Conf. Ser.* (2017) 850: 012023.
- (40) Szalai A, Sipos Á, Csapó E, Hornok V, Tóth L, Csete M and Dékány I. Numerical investigation of the plasmonic properties of bare and cysteine-functionalized silver nanoparticles. *Proc. SPIE* (2011) 8096: 80963B-1.
- (41) Szalai A, Sipos Á, Csapó E, Tóth L, Csete M and Dékány I. Comparative study of plasmonic properties of cysteine-functionalized gold and silver nanoparticle aggregates. *Plasmonics* (2013) 8: 53–62.
- (42) Baranova OA, Khizhnyak SD and Pakhomov PM. Supramolecular hydrogel based on L-cysteine and silver nanoparticles. *J. Struct. Chem.* (2014) 55: 169-74.
- (43) Maeda H, Wu J, Sawa T, Matsumura Y and Hori K. Tumor vascular permeability and the EPR effect in macromolecular therapeutics: a review. *J. Control Release* (2000) 65: 271-84.
- (44) Alexis F, Pridgen E, Molnar LK and Farokhzad OC. Factors affecting the clearance and biodistribution of polymeric nanoparticles. *Mol. Pharm.* (2008) 5: 505-15.
- (45) Singh R and Lillard JW Jr. Nanoparticle-based targeted drug delivery. *Exp. Mol. Pathol.* (2009) 86: 215-23.
- (46) Choi SH, Byeon HJ, Choi JS, Thao L, Kim I, Lee ES, Shin BS, Lee KC and Youn YS. Inhalable self-assembled albumin nanoparticles for treating drug-resistant lung cancer. *J. Control Release* (2015) 197: 199–207.
- (47) Lim SM, Kim TH, Jiang HH, Park CW, Lee S, Chen X and Lee KC. Improved biological half-life and anti-tumor activity of TNF-related apoptosis-inducing ligand (TRAIL) using PEG-exposed nanoparticles. *Biomaterials* (2011) 32: 3538-46.
- (48) Dos Santos KC, da Silva MF, Pereira-Filho ER, Fernandes JB, Polikarpov I and Form MR. Polymeric nanoparticles loaded with the 3,5,3'-triiodothyroacetic acid (Triac), a thyroid hormone: factorial design, characterization, and release kinetics. *Nanotechnol. Sci. Appl.* (2012) 5: 37-48.
- (49) Vaculová A, Hofmanová J, Soucek K and Kozubik A. Different modulation of TRAIL-induced apoptosis by inhibition of pro-survival pathways in

- TRAIL-sensitive and TRAIL-resistant colon cancer cells. *FEBS Lett.* (2006) 580: 6565–9.
- (50) Ashkenazi A. Targeting death and decoy receptors of the tumornecrosis factor superfamily. *Nat. Rev. Cancer* (2002) 2: 420–30.
- (51) Herbst RS, Eckhardt SG, Kurzrock R, Ebbinghaus S, O'Dwyer PJ, Gordon MS, Novotny W, Goldwasser MA, Tohnya TM, Lum BL, Ashkenazi A, Jubb AM and Mendelson DS. Phase I dose-escalation study of recombinant human Apo2L/TRAIL, a dual proapoptotic receptor agonist, in patients with advanced cancer. *J. Clin. Oncol.* (2010) 28: 2839-46.
- (52) Soria JC, Smit E, Khayat D, Besse B, Yang X, Hsu CP, Reese D, Wiezorek J and Blackhall F. Phase 1b study of dulanermin (recombinant human Apo2L/TRAIL) in combination with paclitaxel, carboplatin, and bevacizumab in patients with advanced non-squamous non-small-cell lung cancer. *J. Clin. Oncol.* (2010) 28: 1527-33.
- (53) Kim TH, Jo YG, Jiang HH, Lim SM, Youn YS, Lee S, Chen X, Byun Y and Lee KC. PEG-transferrin conjugated TRAIL (TNF-related apoptosis-inducing ligand) for therapeutic tumor targeting. *J. Control. Release* (2012) 162: 422–8.
- (54) Munshi A, McDonnell TJ and Meyn RE. Chemotherapeutic agents enhance TRAIL-induced apoptosis in prostate cancer cells. *Cancer Chemother. Pharmacol.* (2002) 50: 46–52.
- (55) Vaculová A, Hofmanová J, Andera L and Kozubík A. TRAIL and docosahexaenoic acid cooperate to induce HT-29 colon cancer cell death. *Cancer Lett.* (2005) 229: 43–8.
- (56) Yang X, Li Z, Wu Q, Chen S, Yi C and Gong C. TRAIL and curcumin codelivery nanoparticles enhance TRAIL-induced apoptosis through upregulation of death receptors. *Drug Deliv.* (2017) 24: 1526–36.
- (57) Ganten TM, Koschny R, Sykora J, Schulze-Bergkamen H, Büchler P, Haas TL, Schader MB, Untergasser A, Stremmel W and Walczak H. Preclinical differentiation between apparently safe and potentially hepatotoxic applications of TRAIL either alone or in combination with chemotherapeutic drugs. *Clin. Cancer Res.* (2006) 12: 2640-6.
- (58) Li F, Guo Y, Han L, Duan Y, Fang F, Niu S, Ba Q, Zhu H, Kong F, Lin C and Wen X. *In-vitro* and *in-vivo* growth inhibition of drug-resistant ovarian carcinoma cells using a combination of cisplatin and a TRAIL-encoding retrovirus. *Oncol. Lett.* (2012) 4: 1254–8.
- (59) Bangert A, Cristofanon S, Eckhardt I, Abhari BA, Kolodziej S, Hacker S, Vellanki SH, Lausen J, Debatin KM and Fulda S. Histone deacetylase inhibitors sensitize glioblastoma cells to TRAIL-induced apoptosis by c-myc-mediated downregulation of cFLIP. *Oncogene* (2012) 31: 4677–88.
- (60) Jiang HH, Kim TH, Lee S, Chen X, Youn YS and Lee KC. PEGylated TNF-related apoptosis-inducing ligand (TRAIL) for effective tumor combination therapy. *Biomaterials* (2011) 32: 8529-37.
- (61) Kim TH, Youn YS, Jiang HH, Lee S, Chen X and Lee KC. PEGylated TNF-Related Apoptosis-inducing ligand (TRAIL) analogues: pharmacokinetics and antitumor effects. *Bioconjug. Chem.* (2011) 22: 1631-7.
- (62) Lim SM, Kim TH, Jiang HH, Park CW, Lee S, Chen X and Lee KC. Improved biological half-life and anti-tumor activity of TNF-related apoptosis-inducing ligand (TRAIL) using PEG-exposed nanoparticles. *Biomaterials* (2011) 32: 3538-46.
- (63) Ke S, Zhou T, Yang P, Wang Y, Zhang P, Chen K, Ren L and Ye S. Gold nanoparticles enhance TRAIL sensitivity through Drp1-mediated apoptotic and autophagic mitochondrial fission in NSCLC cells. *Int. J. Nanomedicine* (2017) 12: 2531-51.
- (64) Huang YJ and Hsu SH. TRAIL-functionalized gold nanoparticles selectively trigger apoptosis in polarized macrophages. *Nanotheranostics* (2017) 1: 326-36.
- (65) Müller N, Schneider B, Pfizenmaier K and Wajant H. Superior serum half life of albumin tagged TNF ligands. *Biochem. Biophys. Res. Commun.* (2010) 396: 793–9.
- (66) Bae S, Ma K, Kim TH, Lee ES, Oh KT, Park ES, Lee KC and Youn YS. Doxorubicin-loaded human serum albumin nanoparticles surface-modified with TNF-related apoptosis-inducing ligand and transferrin for targeting multiple tumor types. *Biomaterials* (2012) 33: 1536-46.
- (67) Kim H, Jeong D, Kang HE, Lee KC and Na K. A sulfate polysaccharide/TNF-related apoptosis-inducing ligand (TRAIL) complex for the long-term delivery of TRAIL in poly(lactic-co-glycolic acid) (PLGA) microspheres. *J. Pharm. Pharmacol.* (2013) 65: 11–21.
- (68) Rudner J, Jendrossek V, Lauber K, Daniel PT, Wesselborg S and Belka S. Type I and type II reactions in TRAIL-induced apoptosis -- results from dose–response studies. *Oncogene* (2005) 24: 130-40.